Measurement of the rate of change of the electron heat flux due to the whistler instability with Solar Orbiter observations

Jesse Coburn[1], Daniel Verscharen[1], Christopher Owen[1], Timothy Horbury[2], Milan Maksimovic[3], Christopher H.K. Chen[4], Fan Guo[5], and Xiangrong Fu[6,7]

[1] MSSL, University College London, Dorking, UK, [2] Department of Physics, Imperial College London, London, UK, [3] LESIA, Observatoire de Paris, Universite PSL, CNRS, Sorbonne Universite, Universite de Paris, Meudon, France, [4] Department of Physics and Astronomy, Queen Mary University of London, London, UK, [5] Los Alamos National Laboratory, Theoretical Division, Los Alamos, NM, USA, [6] New Mexico Consortium, Los Alamos, NM , USA, [7] Los Alamos National Laboratory, Los Alamos, NM , USA

The study of solar wind electrons

- Coronal electrons that are non-Maxwellian contribute to solar wind acceleration and the solar wind thermal energy budget through the gradient of the heat flux.
- Collisions, large-scale fields, turbulent mesoscale electromagnetic fields, and instabilities shape the electron velocity distribution function (VDF).
- Observations of solar wind electrons are dominated by a Maxwellian core (%90) and three non-Maxwellian features: strahl - a field-aligned beam, halo - isotropic super thermal electrons, deficit - sunward absence of phase space density.
- Non-Maxwellian features in the electron VDF can destabilise the plasma, causing plasma wave emission at the expense of particle energy, softening the non-Maxwellian features.
- This project directly measures the rate of change of macroscopic quantities (e.g. temperature and heat flux) according to quasilinear theory using Solar Orbiter observations.

Quasilinear theory

Following Marsch et al. 2006, the quasilinear equations are written,

Wave frame pitch-angle gradient

$$(1)\quad \frac{\partial}{\partial t}F_s(t,v_\parallel,v_\perp)=\frac{1}{(2\pi)^3}\int_{-\infty}^{\infty}\mathrm{d}^3k\;\underbrace{\hat{\mathscr{B}}(k_i)}_{\text{Magnetic field energy spectrum}}\frac{1}{v_\perp}\frac{\partial}{\partial\alpha}v_\perp\underbrace{\nu_s(k_i,v_\parallel,v_\perp)}_{\text{Resonance condition}}\frac{\partial}{\partial\alpha}F_s(t,v_\parallel,v_\perp),$$

Spatially averaged VDF

The wave frame pitch-angle gradient,

$$(2)\quad \frac{\partial}{\partial\alpha}=v_\perp\frac{\partial}{\partial v_\parallel}+\left[v_{\mathrm{phase}}(k_i)-v_\parallel\right]\frac{\partial}{\partial v_\perp},\quad \text{where the phase speed is } v_{\mathrm{phase}}(k_i)=\omega(k_i)/k_\parallel.$$

The resonant speed, $(3)\quad V_s(k_i,p)=\dfrac{\omega(k_i)-p\,\Omega_s}{k_\parallel}$, and $V'_s(k_i,p)=\dfrac{\omega'(k_i)-p\,\Omega_s}{k_\parallel}+u_\parallel^s$,

Moments of Equation (1) produce,

$$(4)\quad \frac{\partial}{\partial t}\begin{Bmatrix}n_su_\parallel^s\\P_\parallel^s\\P_\perp^s\\q_\parallel^s\\q_\perp^s\end{Bmatrix}=\frac{\Omega_s^2}{(2\pi)^3}\int_{-\infty}^{\infty}\mathrm{d}^3k\;\hat{\mathscr{B}}(k_i)\frac{1}{k_\parallel}\sum_{p=-\infty}^{\infty}\int_0^\infty\mathrm{d}v_\perp\,\mathscr{R}_s(k_i,p)\begin{Bmatrix}1\\2m_sV'_s(k_i,p)\\pm_s\Omega_s/k_\parallel\\3m_sV'_s(k_i,p)^2\\\dfrac{m_s}{2}\left(v_\perp^2+2\dfrac{p\Omega_s}{k_\parallel}V'_s(k_i,p)\right)\end{Bmatrix}+\begin{Bmatrix}0\\0\\0\\-3p_\parallel^s\,\partial u_\parallel^s/\partial t\\-p_\perp^s\partial u_\parallel^s/\partial t\end{Bmatrix}$$

$$(5)\quad \text{The resonance function: }\quad \mathscr{R}_s(k_i,p)\propto\left(-\frac{\partial}{\partial\alpha}F_s(t,v_\parallel,v_\perp)\right)_{v_\parallel=V_s(k_i,p)}$$

The collective equations describe the rate of change of the macroscopic quantities. The key measurements are the wave frame pitch-angle gradient and the magnetic field energy spectrum.

Solar Orbiter observations

- The observations are the same interval studied in Berčič et al. 2021:
  - June 24, 2020 while Solar Orbiter was at a heliocentric distance of 112 solar radii a short bandwidth enhancement of electromagnetic fluctuations were detected by the Radio and Plasma Waves instrument.
  - The Solar Wind Analyser measured an electron distribution function displaying a deficit and strahl.
  - The electromagnetic enhancement is between the proton and electron cyclotron frequencies, quasi-parallel to the magnetic field (3.8°), and the wave ellipticity of the bandwidth is > 0.5. They are quasi-parallel right hand circularly polarised whistler waves.

This project analyses the same interval to directly show the wave-particle interaction is occurring and measure the rate of change of the macroscopic quantities. This is done by obtaining gradients of the electron VDF: the primary novel piece of the analysis.

The analysis method

- Remove low energy electrons and fill with a Maxwellian fit.
- Interpolate the VDF to regular $v_\perp$, $v_\parallel$ coordinates to take gradients in accordance with the theory.
- A spectral method is considered for the electron VDF to deal with noise and compute smooth gradients. For example, an expansion can be considered,

$$f(x)=\sum_n c_n\Gamma_n(x)\quad \text{And since the functions } \Gamma_n(x) \text{ are}$$

orthonormal the coefficients c_n can be obtained,

$$\int_0^\infty \mathrm{d}x\;\Gamma_m(x)f(x)=\sum_n c_n\int_0^\infty \mathrm{d}x\;\Gamma_m(x)\Gamma_n(x)=\sum_n c_n\delta_{nm}=c_m.$$

- **Legendre-Laguerre transform**
  - The Legendre transform of the electron VDF in normalised parallel velocity $\hat{v}_\parallel=\sqrt{2E/m_e}\,\hat{b}_iv_i/|v_i|$, where E is the energy, m_e is the electron mass, $\hat{b}_i=b_i/|b_j|$ is the normalised magnetic field vector.
  - Take the Laguerre transform of the electron VDF in energy (E).
- The spectra are analysed for a noise floor and truncated appropriately.
- The inverse transform provides a low-pass filtered electron VDF.
- The electron VDF is interpolated to a regular $v_\parallel$, $v_\perp=\sqrt{v_i^2-v_\parallel^2}$ grid

so that it can be treated with quasilinear theory.

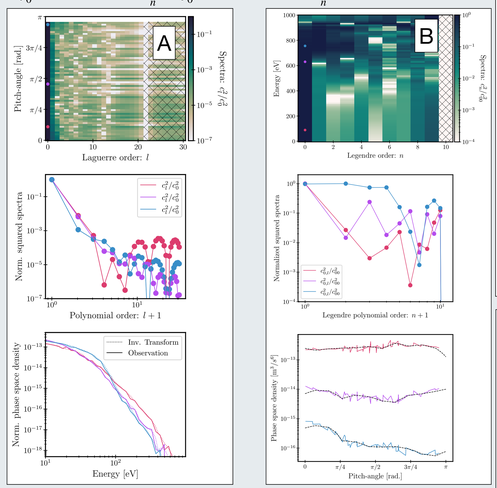

Low-pass filter in velocity space

Figure A: (Top left) at each pitch-angle the Laguerre transform in energy is shown as the color bar. Hashed portion is set to zero. (Middle) line plot of the squared Laguerre spectra, color maps to dots on top left panel. (Bottom) comparison of the inverse transformed function and the observation.

Figure B: (Top) at each energy the Legendre transform in pitch-angle is shown as the color bar. Hashed portion is set to zero. (Middle) line plot of the square Legendre spectra, color maps to dots on the top panel. (Bottom) comparison of the inverse transformed function and the observation.

Figure C: (Top left) the inverse transformed VDF interpolated to $v_\perp$, $v_\parallel$. (Top right) before interpolation, black dots mark the grid in E, pitch-angle. (Bottom left) bi-Maxwellian comparison. (Bottom right) normalized difference between the interpolated function and the bi-Maxwellian.

Figure D: (Top left) perpendicular derivative of the interpolated transformed function. (Top right) parallel derivative of the interpolated transformed function. (Bottom left) perpendicular derivative of the bi-Maxwellian function. (Bottom right) parallel derivative of the bi-Maxwellian function.

Figure E: (Left column) parallel slice along magenta lines in Figure C. (Right column) perpendicular slice along magenta lines in Figure C.

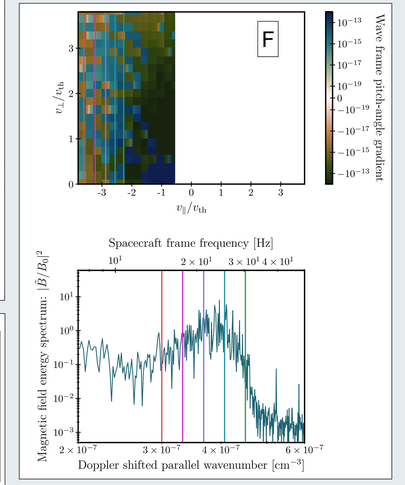

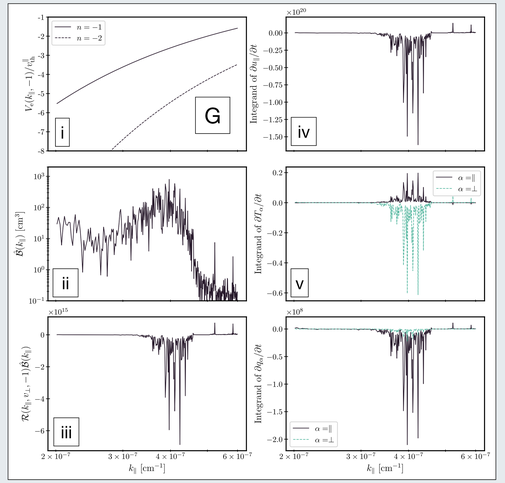

Wave-frame pitch-angle gradient

Figure F: (Top) Eqn. 2 of the interpolated and transformed electron VDF analysed at the resonant velocity Eqn. 3, i.e. $v_\parallel=V_s(k_\parallel,-1)$. Vertical coloured lines map to the bottom panel via the resonant velocity (Eqn. 3) and Doppler shift. (Bottom) the magnetic field energy spectrum observed by the Radio and Plasma Waves instrument on Solar Orbiter. The Doppler shift is computed by inverting:

$$\omega_{\mathrm{sc}}=\omega_{\mathrm{whistler}}+|\mathbf{k}|\,|\mathbf{V}_{\mathrm{SW}}|\cos\left(\theta_{k,V}\right),$$

where ω_{sc} is the spacecraft frequency, $\omega_{\mathrm{whistler}}$ is the dispersion relation, $\mathbf{k}$ is the wavenumber, $\mathbf{V}_{\mathrm{SW}}$ is the solar wind velocity, $\theta_{k,V}$ is the angle between the wave and the solar wind.

Figure G: (i) Resonant velocities (Eqn. 3). (ii) Unnormalised magnetic field energy spectrum. (iii) The essential part of the integrand in Eqn. 4. (iv) Rate of change of the parallel bulk velocity (Eqn. 5). (v) Rate of change of the parallel temperature (Eqn. 5). (vi) Rate of change of the heat flux (Eqn. 5).

Conclusions and future work

- Quasilinear theory has been extended to measure the rate of change of the heat flux due to resonant wave-particle interactions.
- A low-pass filter in velocity space of the VDF has been constructed to obtain the wave frame pitch-angle gradient and remove noise.
- This method has been applied to Solar Orbiter measurements of the electron VDF by SWA and the magnetic field by RPW.
- There is a loss of momentum and the temperatures are becoming more isotropic. The parallel electron heat flux is decreasing.
- This is a direct measurement of the wave-particle interaction and the first time the decrease of the heat flux has been measured.
- The low pass filter technique is not meeting expectations, but when ready, it can be applied to obtain the velocity space gradient, which governs all electromagnetic and collisional interactions.

Contact details for Jesse Coburn: j.coburn@ucl.ac.uk